ARTICLE
Traditional Medicine Research 2026;11(2):8. https://doi.org/10.53388/TMR20240618002

Investigating the potential mechanisms of Wenqing Yin against atopic dermatitis based on network pharmacology, experimental pharmacology, and molecular docking

Yi Wang[1], Zhen Liu[1], Si-Man Li[1], Lin Lin[1], Wei Dai[2*], Meng-Yue Ren[1*]

[1]School of Traditional Chinese Medicine, Guangdong Pharmaceutical University, Guangzhou 510006, China. [2]Experiment Center of Teaching, Guangdong Pharmaceutical University, Guangzhou 510006, China.

[*]**Correspondence to:** Wei Dai, Experiment Center of Teaching, Guangdong Pharmaceutical University, No. 280, Waihuan East Road, Guangzhou 510006, China. E-mail: dai_gdpu_2018@gdpu.edu.cn. Meng-Yue Ren, School of Traditional Chinese Medicine, Guangdong Pharmaceutical University, No. 280, Waihuan East Road, Guangzhou 510006, China. E-mail: Rmy0711@163.com.

Author contributions

Wei D designed the experiments and analyzed the data; Ren MY designed the experiments, analyzed the data, and revised the manuscript; Wang Y wrote the manuscript and analyzed the data; Wang Y, Liu Z, Li SM and Lin L performed the experiments. All the authors have read and approved the final manuscript.

Competing interests

The authors declare no conflicts of interest.

Acknowledgments

This work was supported by grants from the National Natural Science Foundation of China (82004252), the Project of Administration of Traditional Chinese Medicine of Guangdong Province (20240511201759650O) and the Basic and Applied Basic Research Foundation of Guangzhou Municipal Science and Technology Bureau (202102020533).

Peer review information

Traditional Medicine Research thanks Peng Lin and other three anonymous reviewers for their contribution to the peer review of this paper.

Abbreviations

WQY, Wenqing Yin; AD, atopic dermatitis; TCM, traditional Chinese medicine; DNFB, 2,4-dinitrofluorobenzene; QRT-PCR, quantitative real-time-polymerase chain reaction; HE, hematoxylin-eosin; UPLC-MS/MS, ultra-performance liquid chromatography-tandem mass spectrometry; IL-6, interleukin-6; Th, T helper; SPF, specific pathogen-free; WQY-L, low-concentration WQY; WQY-H, high-concentration WQY; TEWL, transcutaneous water loss; FITC, fluorescein isothiocyanate; BV421, Brilliant Violet 421; APC, allophycocyanin; PPI, protein-protein interaction; KEGG, Kyoto Encyclopedia of Genes and Genomes; GO, Gene Ontology; MF, molecular functions; BP, biological processes; CC, cellular components; PPI, protein-protein interaction.

Citation

Wang Y, Liu Z, Li SM, Lin L, Dai W, Ren MY. Investigating the potential mechanisms of Wenqing Yin against atopic dermatitis based on network pharmacology, experimental pharmacology, and molecular docking. *Tradit Med Res*. 2026;11(2):8. doi: 10.53388/TMR20240618002.

Executive editor: Feng Wang.

Received: 18 June 2024; **Revised:** 30 January 2025; **Accepted:** 23 April 2025; **Available online**: 25 April 2025.

Abstract

Background: Wenqing Yin (WQY) is a classic prescription used to treat skin diseases like atopic dermatitis (AD) in China, and the aim of this study is to investigate the therapeutic effects and molecular mechanisms of WQY on AD. **Methods:** The DNFB-induced mouse models of AD were established to investigate the therapeutic effects of WQY on AD. The symptoms of AD in the ears and backs of the mice were assessed, while inflammatory factors in the ear were quantified using quantitative real-time-polymerase chain reaction (qRT-PCR), and the percentages of $CD4^+$ and $CD8^+$ cells in the spleen were analyzed through flow cytometry. The compounds in WQY were identified using ultra-performance liquid chromatography-tandem mass spectrometry (UPLC-MS/MS) analysis and the key targets and pathways of WQY to treat AD were predicted by network pharmacology. Subsequently, the key genes were tested and verified by qRT-PCR, and the potential active components and target proteins were verified by molecular docking. **Results:** WQY relieved the AD symptoms and histopathological injuries in the ear and back skin of mice with AD. Meanwhile, WQY significantly reduced the levels of inflammatory factors IL-6 and IL-1β in ear tissue, as well as the ratio of $CD4^+/CD8^+$ cells in spleen. Additionally, a total of 142 compounds were identified from the water extract of WQY by UPLC-Orbitrap-MS/MS. 39 key targets related to AD were screened out by network pharmacology methods. The KEGG analysis indicated that the effects of WQY were primarily mediated through pathways associated with Toll-like receptor signaling and T cell receptor signaling. Moreover, the results of qRT-PCR demonstrated that WQY significantly reduced the mRNA expressions of IL-4, IL-10, GATA3 and FOXP3, and molecular docking simulation verified that the active components of WQY had excellent binding abilities with IL-4, IL-10, GATA3 and FOXP3 proteins. **Conclusion:** The present study demonstrated that WQY effectively relieved AD symptoms in mice, decreased the inflammatory factors levels, regulated the balance of $CD4^+$ and $CD8^+$ cells, and the mechanism may be associated with the suppression of Th2 and Treg cell immune responses.

Keywords: Wenqing Yin; atopic dermatitis; mouse model; UPLC-Orbitrap-MS/MS; network pharmacology

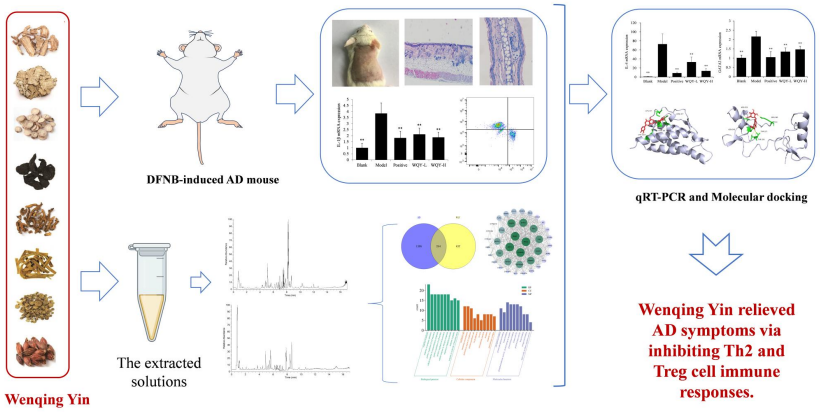

Traditional Medicine Research 2026;11(2):8. https://doi.org/10.53388/TMR20240618002

Highlights

Wenqing Yin ameliorates AD.
Wenqing Yin regulates Th2 and Treg cells immune response.
13 compounds from Wenqing Yin exhibited good binding affinities with IL-4, IL-10, GATA3 and FOXp3 using molecular docking.

Medical history of objective

Wenqing Yin, a classic formula for treating skin inflammation, is derived from Gong Tingxian's "*Wanbing Huichun Volume 6*" (1522 C.E.). In ancient times, Wenqing Yin was often used to promote blood circulation and detoxify. In current studies, modern pharmacological researches have shown that Wenqing Yin has anti-ulcer, anti-inflammation, immune regulation and other effects.

Background

Atopic dermatitis (AD), commonly referred to as atopic eczema, is a prevalent hereditary chronic inflammatory skin condition characterized by pruritus that can manifest on any area of the body. The symptoms of AD are dry skin, itching, red rashes, skin exudation of pus, and skin lichenification, and AD seriously reduces the quality of life of the patients [1, 2]. AD affects a wide range of people with a global prevalence of 2.2% to 17.6% and involves people of all ages. The prevalence rates of AD in children aged 0–17 years, adults aged 18–74 years, and elderly over 75 years old are 18.3%, 7.7%, and 11.6%, respectively [3, 4]. AD usually leads to the occurrence of a series of allergic diseases, up to 60% and 30% of patients with AD will suffer from allergic rhinitis and food allergy, respectively [5]. At present, Western medicine predominantly uses moisturizing agents combined with corticosteroids and calcineurin inhibitors in the treatment of AD, which is effective. However, prolonged administration of corticosteroids may result in muscle atrophy and impaired wound healing. When using calcineurin inhibitors, local burning sensation and increased susceptibility to the virus are observed, and limitations in clinical use are present [6]. Therefore, seeking safe and effective treatments to alleviate AD is still urgent. Traditional Chinese medicine (TCM) has the characteristics of many active ingredients, mild effects, and small side effects, which allows us to find more effective drugs for AD treatment [7]. The TCM-derived compound Wenqing Yin (WQY) is clinically used to treat skin diseases like AD, and modern pharmacological studies have demonstrated that WQY exhibits multiple properties, including anti-ulcer, anti-inflammation, immunoregulation, and other forth [8]. WQY came from the "Wanbing Huichun" written by Gong Tingxian in the Ming Dynasty. WQY is a combination of Siwu Decoction and Huanglian Jiedu Decoction and also known as Jiedu Siwu Decoction, which comprises eight components: *Angelicae Sinensis Radix* (Danggui), *Paeoniae Radix Alba* (Baishao), *Rehmanniae Radix Praeparata* (Shudihuang), *Chuanxiong Rhizoma* (Chuanxiong), *Coptidis Rhizoma* (Huanglian), *Scutellariae Radix* (Huangqin), *Phellodendri Chinensis Cortex* (Huangbo), and *Gardeniae Fructus* (Zhizi). WQY has long been used to treat metrorrhagia and is now frequently used to treat a range of skin disorders. Numerous clinical studies have demonstrated that WQY exhibits a favorable therapeutic effect on AD [9–12]. Nevertheless, additional extensive studies are necessary to investigate the potential of WQY as a treatment for AD and to uncover the mechanisms by which it operates.

In this study, we kindly investigated the therapeutic effects of WQY on AD using a mouse model induced by 2,4-dinitrofluorobenzene (DNFB). We identified and analyzed the chemical components present in WQY through UPLC-Orbitrap-MS/MS, and then explored the molecular mechanisms underlying the action of WQY in treating AD utilizing network pharmacology. Finally, the key genes were tested and verified by qRT-PCR, and the potential active components and target proteins were verified by molecular docking.

Materials and methods

Animals

Sixty specific pathogen-free (SPF) BALB/c male mice, each aged between 7 and 8 weeks, weighing between 18 and 22 g, were acquired from the Laboratory Animal Center of Southern Medical University (Certificate number SCXK 2016-0041). The mice were acclimatized to their environment through a one-week adaptive feeding period prior to the experiment. This study received approval from the Undergraduate Laboratory Animal Center of Guangdong Pharmaceutical University (Approval number gdpulac2021066).

Drug and reagents

DNFB was purchased from Shanghai McLean Biochemical Technology Co., Ltd. (Shanghai, China). Physiological saline was supplied by Zhejiang Tianrui Medicine Co., Ltd. (Ruian, China). Dexamethasone was a product from Shanghai Mao Kang Co., Ltd. (Shanghai, China). TRIzol reagent was obtained from Invitrogen (Carlsbad, CA, USA). Prime Script RT reagent Kit and TB Green Premix Ex Taq II were acquired from TaKaRa (Osaka, Japan).

Huangbo (batch number: YPB0J0002) was purchased from Chinese Herbal Pieces Factory of Guangzhou Medicinal Materials Company (Guangzhou, China). Huanglian (batch number: 20200613) and Chuanxiong (batch number: 20201009) were provided by Kunming Lanhai Chinese Herbal Medicine Pieces Co., Ltd. (Kunming, China). Zhizi (batch number: HX20D01) and Danggui (batch number: HX21M01) were produced by Guangzhou Hexiang Pharmaceutical Co., Ltd. (Guangzhou, China). Huangqin (batch number: 2011022), Baishao (batch number: 201201), and Shoudihuang (batch number: 201101-13) were sourced from Zhongshan Xianyitang traditional Chinese medicine (TCM) Pieces Co., Ltd. (Zhongshan, China), Guangzhou Zhixin Chinese Herbal Medicine Co., Ltd. (Guangzhou, China), and Guangdong Zihetang Pharmacy Co., Ltd. (Guangzhou, China), respectively.

Sample preparation

8 herbs of WQY 15 g each were weighed, added 12 times of water to boil for 30 min, and the filtrate then subjected to a second boiling with 10 times its volume in water for an additional 30 min. Subsequently, the filtrate was concentrated under reduced pressure to achieve concentrations of 1.2 g/mL and 0.6 g/mL. About 2.5 mg of dexamethasone was precisely measured and mixed with 50 mL of distilled water. After ultrasonic mixing, positive drug was obtained.

Preparation of AD mice model and drug administration

A total of 40 BALB/c mice were divided randomly into blank, model, positive, low-concentration WQY (WQY-L), and high-concentration WQY (WQY-H) groups. Under isoflurane anesthesia, the abdomen and back of mice were depilated at a range of 2 cm × 2 cm. Except the blank group, the four other groups were sensitized with 30 μL of 0.5% DNFB solution applied to the abdomen on day 1, and 10 and 50 μL of 0.2% DNFB solution were administered to the right ear and back of mice, respectively, every other day from day 5 to day 21 for challenge. From day 5 to day 21, the positive, WQY-L, and WQY-H groups were given intragastric administration, and blank and model groups were administered with distilled water once a day with a volume of 0.4 mL/20 g.

Measurement of transcutaneous water loss (TEWL) and skin hydration

To measure the TEWL and skin hydration in back skin of mice, we flattened the shaved area on the back of eight mice per group, and touched the skin for 30 s using CK-MPA10 multifunctional skin tester (CK, Cologne, Germany). Each mouse underwent three assessments, and the mean value was calculated.

Evaluation of ear thickness and weight

To evaluate the degree of swelling in the right ear of all mice in each

group, we measured and quantified and analyzed changes in ear thickness and weight. Ear thickness of the right ears was assessed utilizing a thickness gauge (Mitutoyo, Yokohama City, Japan), before sensitization and 24 h following the last challenge. The Equation (1) used is as follows:

Increase in Ear Thickness = Thickness of DNFB-Challenged Right Ear − Thickness of Right Ear before Sensitization (1)

A sterile skin punch (Shanghai, China) was utilized to extract circular tissues with a diameter of 4 mm from the equivalent location of the left and right ears at 24 h after the final challenge. Additionally, the extracted tissues were weighed using the following Equation (2):

Increase in Ear Weight = Weight of DNFB-Challenged Right Ear − Weight of Unchallenged Left Ear (2)

Histopathological examination

A part of the back skin and right ear of eight mice in each group were collected for hematoxylin-eosin (HE) staining. Sections were dewaxed and uniformly stained with aqueous hematoxylin for a few min. Acid and ammonia were then applied to facilitate color separation. Subsequently, the sections were dehydrated using 70% and 90% alcohol for more than 10 min, followed by staining with an alcohol eosin solution for 2 to 3 min. Finally, a few drops of Canada balsam were applied to the already transparent sections. After slicing, histopathological alterations were assessed and documented using a fluorescence microscope (Olympus, Japan).

RNA Isolation and quantitative real-time-polymerase chain reaction (qRT-PCR) analysis

50 mg of ear tissue was added with 0.5 mL of cell lysis buffer. In compliance with the provided instructions, all RNA was extracted from the ear tissue, and both the concentration and purity of the RNA were assessed. Results were recorded. After removing the genomic DNA reaction, instructions were followed to configure the reverse transcription reaction solution, complete the reverse transcription, and store at −20 ˚C. Then, we referenced literature and the National Center for Biotechnology Information designed the primer sequences, and prepared the PCR reaction solution in accordance with the instructions. After the initial denaturation step at 95 ˚C for 5 min, the following thermocycling conditions were employed for the qRT-PCR: followed by 40 cycles of 95 ˚C for 10 s, 55 ˚C for 30 s and 72 ˚C for 20 s. The primer sequences utilized for qRT-PCR are presented in Table 1. All mice were tested for IL-1β and IL-6, while the remaining genes were tested in a random sample of five from each group.

Flow cytometry analysis

Three mice from each group were randomly selected for flow cytometry analysis. The isolated Smooth Muscle Cells (SMCs) were cultured in a 24-well plate and subjected to stimulation with a leukocyte activation cocktail, which comprised phorbol 12-myristate 13-acetate, ionomycin, and brefeldin A. This stimulation was conducted for a duration of 5 h in a humidified CO_2 incubator maintained at 37 ˚C. To prevent non-specific antibody binding through Fc receptors during antibody labelling, the cells were subsequently divided into separate tubes and washed once with PBS, then being treated with an Fc blocking solution at ambient temperature for 15 min. The cells were incubated at ambient temperature for 30 min, protected from light, with fluorescein isothiocyanate (FITC)- and Brilliant Violet 421 (BV421)-conjugated anti-mouse CD4 and CD8 antibodies for surface labeling. After that, the cells were subjected to fixation and permeabilization using an intracellular fixation and permeabilization solution, then were treated at ambient temperature for 15 min without exposure to light with FITC- and allophycocyanin (APC)-labeled anti-mouse CD4 and CD8 antibodies. A FACSCelesta flow cytometer (BD, Franklin Lake, NJ, USA) was used to identify the labelled cells after washing and resuspending them in PBS.

Analysis of the ingredients of WQY by UPLC-MS/MS

The extracted solutions were filtered using 0.22 μm nylon filters and subsequently analyzed via UPLC-Orbitrap-MS/MS (Thermo Fisher Scientific, Waltham, MA, USA). UPLC-MS/MS was performed on an ZORBAX RRHD Eclipse Plus C18 column (2.1 × 100 mm, 1.8 μm) (Agilent, Santa Clara, CA, USA), and the mobile phases of gradient elution for solvents A (0.1% formic acid-water) and B (0.1% formic acid-acetonitrile) were configured as follows: 95%–75% B (0.001–5.000 min), 75%–40% B (5.000–10.000 min), 40%–20% B (10.000–15.000 min), 20%–10% B (15.000–15.001) and 10% B (15.001–17.000). The injection amount was set to 1 μL, while the column was kept at a temperature of 30 ˚C. The following MS conditions were utilized: ESI-both (positive and negative) ion mode, scan Range of 100–800 m/z, RF Lens of 40%, orbital trap resolution of 60,000.

Network pharmacology

Construction and screening of target databases. The UPLC-MS/MS analysis of the WQY revealed 142 prominent compounds. The “sdf” files of compounds were obtained from PubChem database (https://pubchem.ncbi.nlm.nih.gov) and the structures of bioactive compounds were investigated to identify their targets in the Swiss Target Prediction database (http://www.swisstargetprediction.ch) [13, 14]. By using “atopic dermatitis” as search term, AD-related targets were obtained from the DrugBank (https://go.drugbank.com) [15], GeneCards (https://www.genecards.org) [16], and OMIM (https://www.omim.org) databases [17]. The Uniprot database (https://www.uniprot.org) was used to convert gene names [18]. The potential targets associated with AD were determined by integrating information from three databases and eliminating any redundant entries. Subsequently, the intersection targets were identified utilizing Venny 2.1.0 (https://bioinfogp.cnb.csic.es/tools/venny/index.html) [19].

Table 1 Primer sequences for qRT-PCR

Gene	Forward primer (5’-3’)	Reverse primer (5’-3’)
IL-1β	GCAACTGTTCCTGAACTCAACT	ATCTTTTGGGGTCCGTCAACT
IL-6	TAGTCCTTCCTACCCCAATTTCC	TTGGTCCTTAGCCACTCCTTC
IFN-γ	TCAAGTGGCATAGATGTGGAAGAA	TGGCTCTGCAGGATTTTCATG
IL-4	ACAGGAGAAGGGACGCCAT	GAAGCCCTACAGACGAGCTCA
IL-17	GGCCCTCAGACTACCTCAAC	TCTCGACCCTGAAAGTGAAGG
IL-10	GGTTGCCAAGCCTTATCGGA	ACCTGCTCCACTGCCTTGCT
T-bet	AGCAAGGACGGCGAATGTT	GTGGACATATAAGCGGTTCCC
GATA3	AAGCTCAGTATCCGCTGACG	GTTTCCGTAGTAGGACGGGAC
RORγ	CCTGGGCTCCTCGCCTGACC	TCTCTCTGCCCTCAGCCTTGCC
FOXP3	CACCTATGCCACCCTTATCCG	CATGCGAGTAAACCAATGGTAGA
GAPDH	ACCTGCCAAGTATGATGACATCA	GGTCCTCAGTGTAGCCCAAGAT

Acquisition of key targets and construction of protein-protein interaction (PPI) network. To investigate the PPI of potential targets, the STRING database (https://cn.string-db.org/) was utilized. The species type has been designated as "*Homo sapiens*", and the "interaction score" has been established at "0.900" [20]. The "TSV" file of the PPI network was imported into the Cytoscape 3.7.1 to construct the interaction network diagram and export the corresponding data for topological analysis. Using the Cytoscape plug-in CentiScape, hub node was identified as a key target for AD treatment by applying three thresholds: the median values of closeness, betweenness, and degree centrality. Finally, the key targets were inputted to STRING database to acquire pertinent information regarding protein interactions [21].

Network construction and analysis. The active compounds, key targets, and associated diseases were imported into Cytoscape software to construct a regulatory network diagram titled "WQY-compounds-targets-disease". Additionally, the Network Analyzer plug-in for Cytoscape was employed to analyze the potential relationships between the genes and compounds related to WQY.

Kyoto encyclopedia of genes and genomes (KEGG) pathway enrichment and gene ontology (GO) analysis. The key targets of WQY for AD were submitted to the Metascape database (https://Metascape.org) for GO and KEGG pathway enrichment analysis, with the species type specified as "*Homo sapiens*" [22]. The GO enrichment analysis covered three primary categories: GO molecular functions (MF), GO biological processes (BP), and GO cellular components (CC). Meanwhile, the KEGG enrichment analysis provided insights into genomic information associated with the relevant targets [23]. The findings from both the GO and KEGG enrichment analyses were illustrated using charts generated on the Science and Research online plotting platform (http://www.bioinformatics.com.cn).

Molecular docking analysis

In this study, the potential active components of WQY were selected for molecular simulation verification with IL-4, IL-10, GATA3, and FOXP3 proteins. The active compounds were obtained from the PubChem database and subsequently saved in "mol2" format using OpenBabel software (http://openbabel.org) [24]. The validated protein structures of IL-4, IL-10, GATA3, and FOXP3 were retrieved from the Protein Data Bank (PDB) database (https://www.rcsb.org) [25], and the binding ability was verified with the above 50 compounds. The higher total score (TS) of molecule-target represents the stronger binding ability of the compound to the target, so 13 molecules were selected for more detailed molecular analysis using Autodock Vina software [26]. Finally, Pymol software (https://pymol.org) was utilized for visualisation and analysis.

Statistical analysis

SPSS Statistics version 25.0 was used for data analysis. Calculated data are expressed as mean ± SD, and univariate ANOVA test is used for significance analysis. $P < 0.05$ was considered to indicate a statistically significant difference.

Results and analysis

WQY increased the SC hydration and the TEWL, and relieved the histopathological injuries in back skin of AD mice

Compared to the blank group, SC hydration was significantly reduced and TEWL was markedly increased in the model group. After administration, WQY-L and WQY-H groups showed improvements in back skin keratosis and epidermal thickening, along with a significant increase in SC hydration and a significant decrease in TEWL compared to the model group (Figure 1A–1C). Furthermore, in comparison to the blank group, the epidermis of skin lesions induced by DNFB in mice exhibited thickening, accompanied by infiltration of inflammatory cells within the dermis. After treatment with WQY, the pathological changes were alleviated, and the local thickening induced by DNFB was significantly reduced in the WQY-H group. Compared to the model group, the epidermal thickness of WQY-L group was markedly changed (Figure 1D). The findings suggest that WQY effectively mitigated inflammatory responses in the skin tissue of mice exhibiting AD-like symptoms.

WQY reduced the ear thickness and weight, and relieved the histopathological injuries in ears of AD mice

The increasing in ear thickness and weight were evaluated and analyzed. Compared with the blank group, the increases in ear thickness and weight of the model group were significantly increased, and the stimulated right ear became incrassation and had obvious red bloodline. After administration, WQY-L and WQY-H groups showed less redness in the right ear and significantly less increases in ear thickness and weight than the model group (Figure 2A, 2B). Meanwhile, WQY reduced pathological damage to skin. As presented in Figure 2C, compared with blank group, the dermal blood vessels in the AD mice were dilated and congested, the infiltration of eosinophils

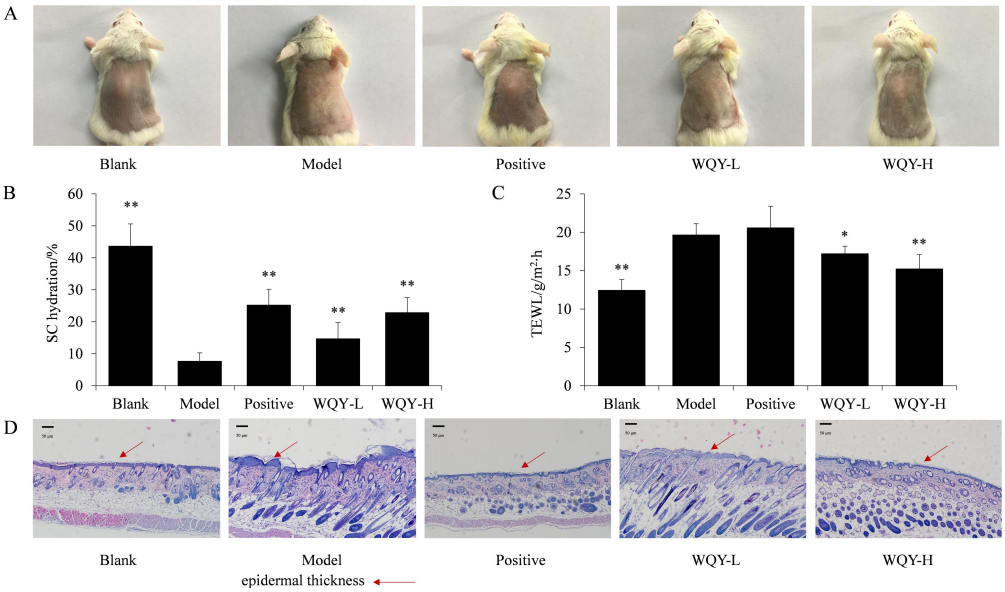

Figure 1 Effect of WQY in back skin of AD mice. At 24 h after the last challenge, (A) the morphology, (B) stratum corneum (SC) hydration, (C) TEWL, and (D) the histopathological injuries in the back of AD mice. Scale bar = 50 μm. Data are expressed as mean ± SD; n = 8; $^{*}P < 0.05$, $^{**}P < 0.01$ versus model. WQY, Wenqing Yin; AD, atopic dermatitis; TEWL, transcutaneous water loss.

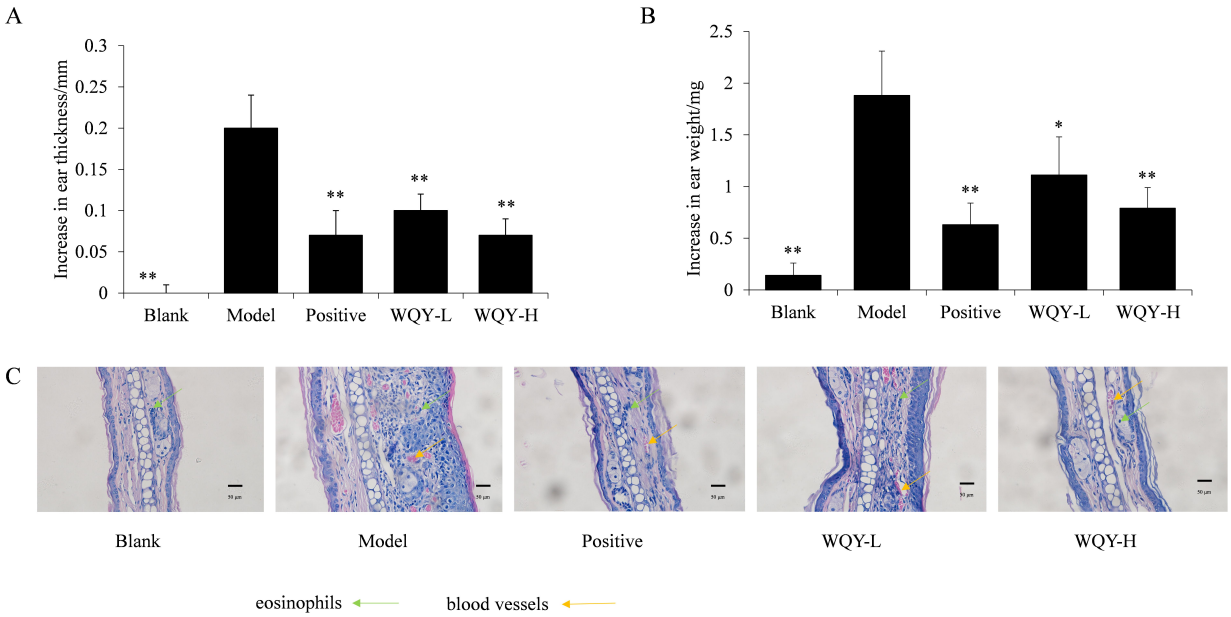

Figure 2 Effect of WQY in ears of AD mice. (A) The increases in ear thickness, (B) the increases in ear weight, and (C) the histopathological injuries in ears of AD mice. Scale bar = 50 μm. Data are expressed as mean ± SD; n = 8; $^{*}P < 0.05$, $^{**}P < 0.01$ versus model. WQY, Wenqing Yin; AD, atopic dermatitis.

increased, and the hair follicle structure was reduced. After WQY treatment, blood vessels in back of AD mice were significantly constricted, and the infiltration of eosinophils decreased.

WQY reduced the mRNA expressions of IL-1β and IL-6 in ears of AD mice

The mRNA expressions of IL-1β and IL-6 in ears of AD mice were measured by qRT-PCR (Figure 3). Relative to the blank group, the mRNA expressions of IL-1β and IL-6 in the model group were significantly upregulated ($P < 0.01$). In comparison to the model group, the mRNA expressions of IL-1β and IL-6 in the WQY-L and WQY-H groups showed a significant reduction ($P < 0.05$; $P < 0.01$).

Effect of WQY on the percentages of $CD4^+$ and $CD8^+$ cells in spleen of DNFB-induced AD mice

The study explored the spleen T cell subpopulations in all groups of mice (Figure 4). The findings revealed that the model group had a substantially elevated $CD4^+/CD8^+$ ratio when compared to the blank group. After the drug interventions, the ratios of $CD4^+/CD8^+$ in positive, WQY-L, and WQY-H groups were markedly decreased to 1.61%, 2.34%, and 2.10% ($P < 0.01$; $P < 0.05$; $P < 0.01$).

The ingredients in WQY by UPLC-MS/MS

As illustrated in Figure 5, the total ion chromatogram (TIC) was obtained using the UPLC-Orbitrap-MS/MS system, operating in both positive mode (A) and negative mode (B). By comparing the results with known chemical components from relevant databases, a total of 142 compounds present in WQY were tentatively identified. These included flavonoids, terpenoids, organic acids, and alkaloids. In the positive ion mode, a total of 78 compounds were identified, whereas in the negative ion mode, 70 compounds were detected. Furthermore, a cumulative total of 142 compounds was observed across both ion modes, with 6 components being detectable in both positive and negative modes. The detailed information on the 142 identified ingredients, including their retention time, ion mode, molecular formula, mass error, and MS/MS fragmentation, were provided in Supplementary Table S1.

Network pharmacology analysis

Construction and screening of target databases. A total of 142 compounds were successfully identified by UPLC-Orbitrap-MS/MS analysis through a comparison with data from the databases and literature, and 691 active targets of WQY were obtained after merging and deleting duplicate values by using the Swiss Target Prediction database. Furthermore, utilizing "atopic dermatitis" as the key term, a total of 1,649 AD-related targets were retrieved and consolidated from the databases of DrugBank, GeneCards, and OMIM. By merging the corresponding targets associated with WQY with those related to AD, we identified a total of 254 intersection targets (Figure 6A).

Acquisition of key targets and construction of PPI network. The PPI network serves as a valuable tool for elucidating BP, CC, and MF. It facilitates the exploration of interactions among target proteins based on data from the STRING database. The visualization of this network, utilizing potential targets as inputs, resulted in a PPI network characterized by diverse interactions. In the subsequent topology analysis conducted using Cytoscape software, nodes meeting three specific thresholds were identified as key targets for AD treatment based on degree (value 7.17), closeness (value 0.09), and betweenness (value 391.07). A total of 39 key targets were identified, such as STAT3, MAPK3 and AKT1, among others. The key targets were incorporated into the STRING database for the construction of the PPI network (Figure 6B). Due to the intricate nature of the PPI, we conducted further analysis on the hub genes and developed a hub gene network. The hub gene network illustrated in Figure 6C proved instrumental in WQY treatment for AD, with pivotal hub genes such as CTNNB1, AKT1, BCL2, and ESR1 playing crucial roles.

The potential ingredients of WQY in treating AD. On the basis of the Cytoscape 3.7.1, we constructed a WQY-compounds-targets-disease network with 91 nodes and 296 edges (Figure 6D, Supplementary Table S2). The purple "V", blue hexagon, green triangle and yellow diamond represented WQY, AD, compounds, and key targets, respectively. The top 10 compounds with literature support were selected, including oxoglaucine, 3,3',4'-trimethoxyflavone, scutellarein 4'-methyl ether, muricarpone B, coumestrol, luteolin, kaempferol, 7-O-methylaromadendrin, dehydroglaucine, and wogonin with degree values of 12, 12, 11, 11, 11, 10, 10, 10, 9, and 8, respectively, indicating that the compounds had an effective effect in treating AD.

The related pathways of WQY in treating AD. GO and KEGG enrichment analysis were conducted on 39 key targets to further explore the mechanisms of WQY in AD treatment. GO and KEGG enrichment analysis were conducted utilizing the Metascape database. A total of 1037 items, including 909 BP, 55 CC, and 73 MF items, were obtained by GO analysis. The top 10 most highly enriched BP, CC, and

MF terms were presented in accordance with *P*-value (Figure 6E). The most enriched terms in BP were response to hormone, response to inorganic substance, positive regulation of cell migration, cellular response to organonitrogen compound, among others. The most enriched CC terms were membrane raft, membrane microdomain, perinuclear region of cytoplasm, and so forth. MF terms included phosphatase binding, protein phosphatase binding, kinase binding, and so forth. A total of 165 KEGG pathways were obtained, and the top 20 most significantly enriched pathways were used to draw a KEGG chart in accordance with *P*-value (Figure 6F). The KEGG enrichment analysis revealed that Toll-like receptor signaling pathway, T cell receptor signaling pathway, Th1 and Th2 cell differentiation, among other pathways, are involved in the treatment of AD with WQY. This suggests that WQY plays a significant role in managing AD by modulating multiple complex biological processes.

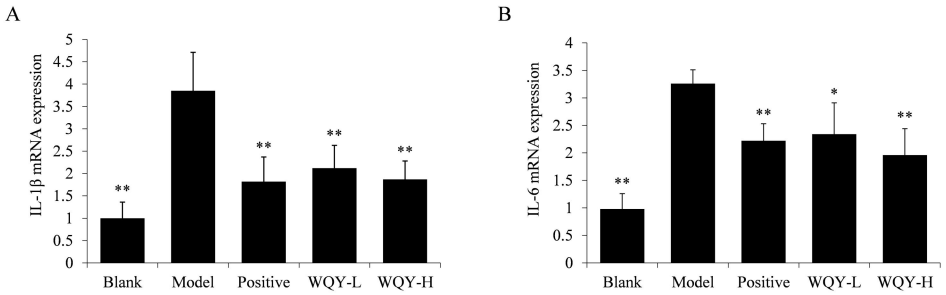

Figure 3 The effect of WQY on the mRNA expressions of IL-1β and IL-6 in ear tissue of AD mice. (A) The mRNA expressions of IL-1β and (B) IL-6. Data are expressed as mean ± SD; n = 8; $^{*}P < 0.05$, $^{**}P < 0.01$ versus model. WQY, Wenqing Yin.

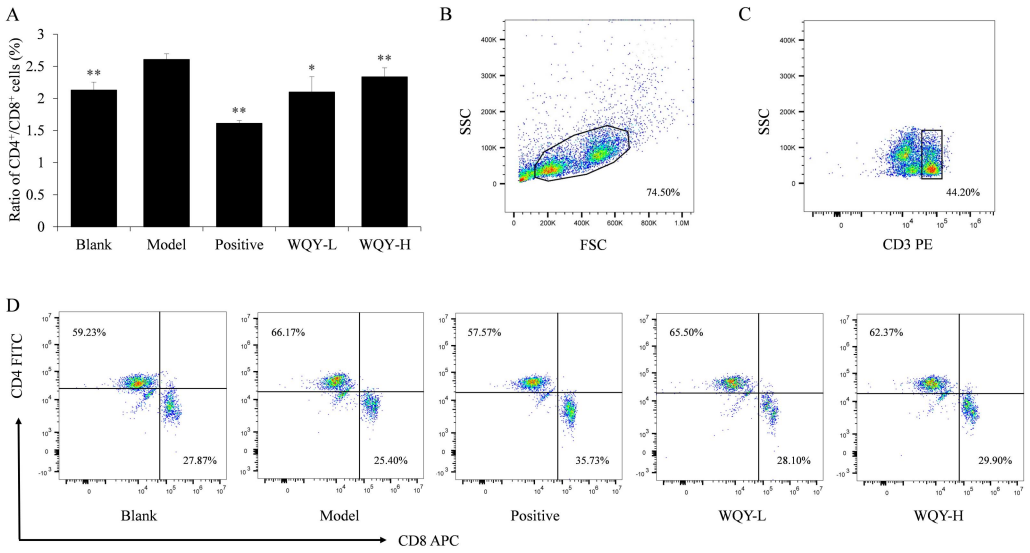

Figure 4 The Effect of WQY on the percentages of $CD4^+$ and $CD8^+$ cells in spleen of DNFB-induced AD mice. (A) The ratio of $CD4^+/CD8^+$ cells, (B) representative dot plots of lymphocyte and (C) CD3 cell, and representative dot plots of $CD4^+$ and $CD8^+$ cells (D). Data are expressed as mean ± SD; n = 3; $^{*}P < 0.05$, $^{**}P < 0.01$ versus model. WQY, Wenqing Yin; FSC, forward scatter; SSC, side scatter.

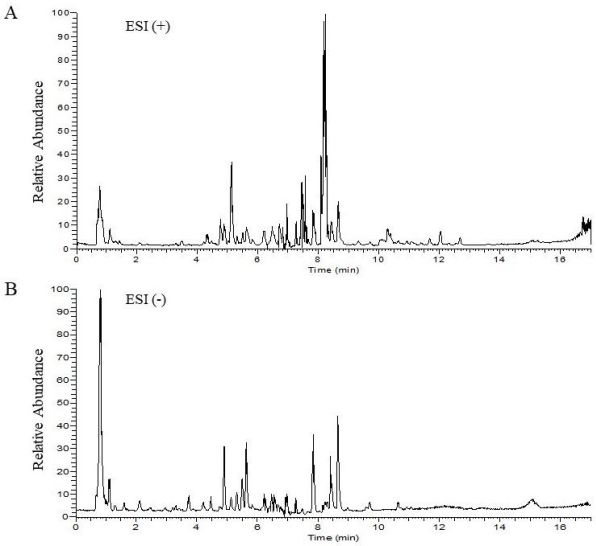

Figure 5 Chromatogram of WQY by UPLC-Orbitrap-MS/MS. (A) Positive-ion polarity mode and (B) Negative-ion polarity mode.

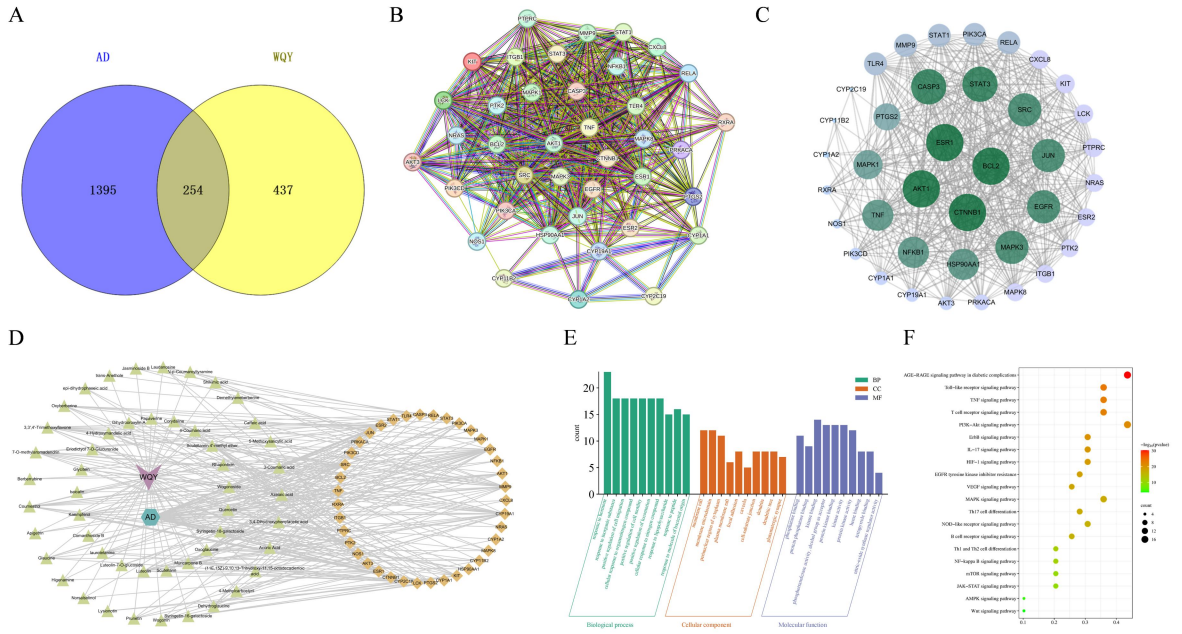

Figure 6 The results of network pharmacology analysis. (A) The venn diagram of the intersection targets of WQY and AD, (B) PPI network of WQY, (C) visual analysis of the PPI network, (D) WQY-compounds-targets-disease network diagram, (E) bubble chart of GO analysis, and (F) bar chart of KEGG analysis. WQY, Wenqing Yin; AD, atopic dermatitis; KEGG, kyoto encyclopedia of genes and genomes; PPI, protein-protein interaction.

WQY inhibited Th2 and Treg cells immune response in DNFB-induced AD mice

Network pharmacological analysis revealed that WQY may be involved in the pathogenesis of DNFB-induced AD mice through Toll-like receptor pathway, T-cell receptor pathway, and Th1 and Th2 cell differentiation. The objective of this research was to explore the involvement of T cells in the aforementioned pathways through the analysis of secreted molecules and transcription factors characteristic of Th1, Th2, Th17, and Treg cell types. The findings revealed that the model group exhibited significantly elevated levels of IL-4, IL-10, GATA3, and FOXP3 mRNA compared to the blank group ($P < 0.01$) (Figure 7). Conversely, the WQY-L and WQY-H groups demonstrated markedly lower levels of IL-4, IL-10, GATA3, and FOXP3 when compared to the model group ($P < 0.01$). Importantly, no significant variations were detected in IFN-γ, IL-17, T-bet, or RORγ mRNA levels among the groups. These findings indicate that the mechanism underlying WQY treatment for AD may be associated with modulating immune functions related to Th2 and Treg cells within these specified pathways.

Results of molecular docking

A study was conducted to investigate WQY component interactions with IL-4, IL-10, GATA3 and FOXP3. It is noteworthy that if the binding energy is ≤ −5.0 kJ/mol, the compound can bind effectively to the protein [27]. Docking results revealed that all the docking molecules had binding energies less than −5.0 kJ/mol (Table 2). The findings suggested a compelling and resolute binding force. The binding energy of eriodictyol 7-O-glucuronide, scutellarin, and wogonoside with proteins was ≤ −30 kJ/mol, indicating their strong protein-binding affinity. Furthermore, compound docking patterns with their respective targets can be observed in Figure 8.

Discussion

WQY, as a classical famous recipe, is now frequently used to treat a range of skin disorders, such as AD. In this study, WQY demonstrated the histopathological injuries of the ear and back skin, reduced the ear swelling and weight, increased the SC hydration and reduced TEWL of back skin in mice of AD. Furthermore, WQY significantly lowered the mRNA expression levels of IL-1β and IL-6 in the ear tissue. IL-1β is a pivotal inflammatory cytokine that promotes the synthesis of additional inflammatory factors such as IL-6, activates neutrophils and phagocytic cells, enhances the production of pro-inflammatory mediators, thereby contributing to or exacerbating the inflammatory response [28]. As a Th2 cytokine, IL-6 plays a crucial role in modulating the body's inflammatory response and is instrumental in promoting the abnormal elevation of various inflammatory factors. Therefore, inhibition of the oversecretion of pro-inflammatory cytokines IL-6 and IL-1β is a limited approach for the treatment of AD [29, 30].

The body's immune function can be determined through the $CD4^+/CD8^+$ ratio, which increases with hyper-immunity and decreases with hypo-immunity [31]. In this study, flow cytometry was employed to quantify the $CD4^+$ and $CD8^+$ cell counts in the spleens, followed by the calculation of the $CD4^+/CD8^+$ ratios. During the treatment of AD, the abnormal increase of $CD4^+/CD8^+$ ratio in AD mice can be inhibited [32]. WQY was observed to significantly decrease the ratio of $CD4^+/CD8^+$ cells in our study, indicating that the mechanism by which WQY exerts its therapeutic effects in AD may related to regulate immune dysfunction by correcting the imbalance of $CD4^+/CD8^+$, and restore the dynamic balance of cellular immunity.

LC is the preferred separation technology for the analysis of active ingredients in TCM, which is suitable for the separation of compounds with different polarities, with high accuracy and good repeatability. MS/MS is a method for identifying unknown compounds or quantifying known substances. After the information of the relative molecular weight of the compound is given by the single-stage mass spectrometry, the quasi-molecular ion is subjected to multi-stage cleavage to obtain the ion fragment peak and obtain the ion fragment information [33]. LC-MS/MS combines the efficient separation ability of liquid chromatography with the qualitative advantages of mass spectrometry, which can determine the structure of compounds with high efficiency and high accuracy. In this study, the chemical constituents in WQY were characterized for the first time using the UPLC-Orbitrap-MS/MS technique under the chromatographic conditions previously established by the group. A total of 142 compounds were subsequently identified in both positive and negative ion modes through a combination of database comparison and software prediction analysis.

Table 2 Binding energy of compounds and targets

Compound	Binding energy (kJ/mol)			
	IL4	IL10	GATA3	FOXP3
(11E,15Z)-9,10,13-Trihydroxy-11,15-octadecadienoic acid	−21.8	−21.8	−23.4	−22.6
Azelaic acid	−21.3	−18.4	−21.3	−22.2
Corydaline	−26.8	−29.3	−31.8	−31.8
Eriodictyol 7-O-Glucuronide	−33.5	−30.5	−37.7	−40.6
Higenamine	−28.0	−28.0	−31.0	−31.4
Jasminoside B	−27.2	−24.3	−31.0	−31.4
Laudanosine	−25.1	−27.6	−27.2	−29.7
Muricarpone B	−21.3	−28.5	−30.1	−30.1
N-p-Coumaroyltyramine	−29.3	−31.4	−28.5	−29.7
Papaverine	−25.1	−28.0	−28.5	−31.4
Rhaponticin	−28.0	−30.5	−31.8	−36.0
Scutellarin	−34.3	−31.8	−36.8	−38.9
Wogonoside	−33.5	−31.8	−34.7	−41.0

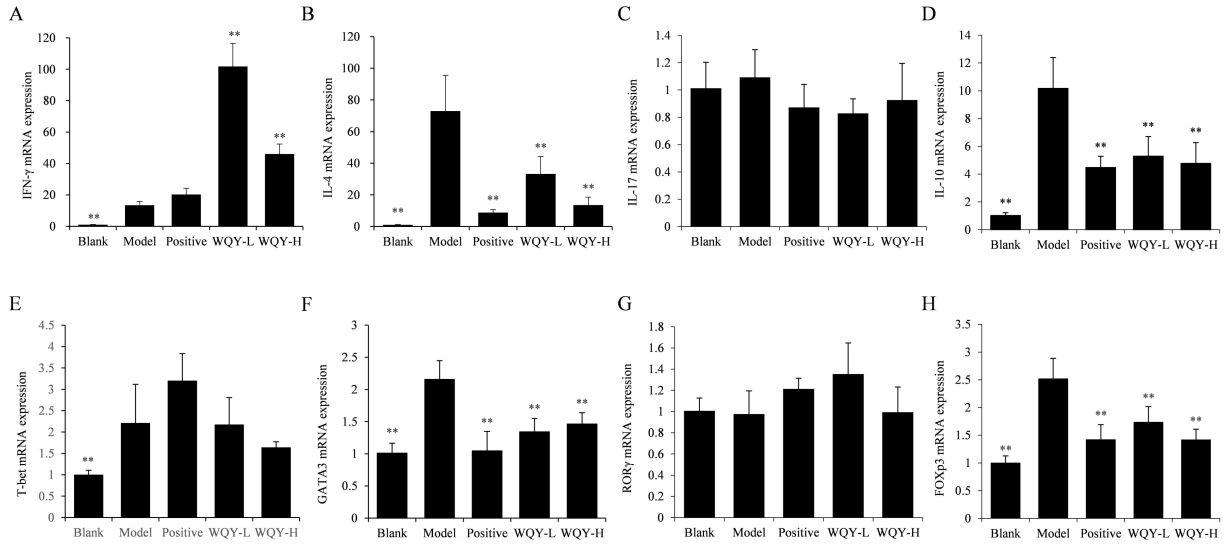

Figure 7 The effect of WQY on the mRNA expression in ears of AD mice. The mRNA expression of (A) *IFN-γ*, (B) *IL-4*, (C) *T-bet*, (D) *GATA3*, (E) *IL-17*, (F) *IL-10*, (G) *RORγ* and (H) *FOXP3* in the ears of AD mice. Data are expressed as mean ± SD; n = 5; $^{*}P < 0.05$, $^{**}P < 0.01$ versus model. WQY, Wenqing Yin.

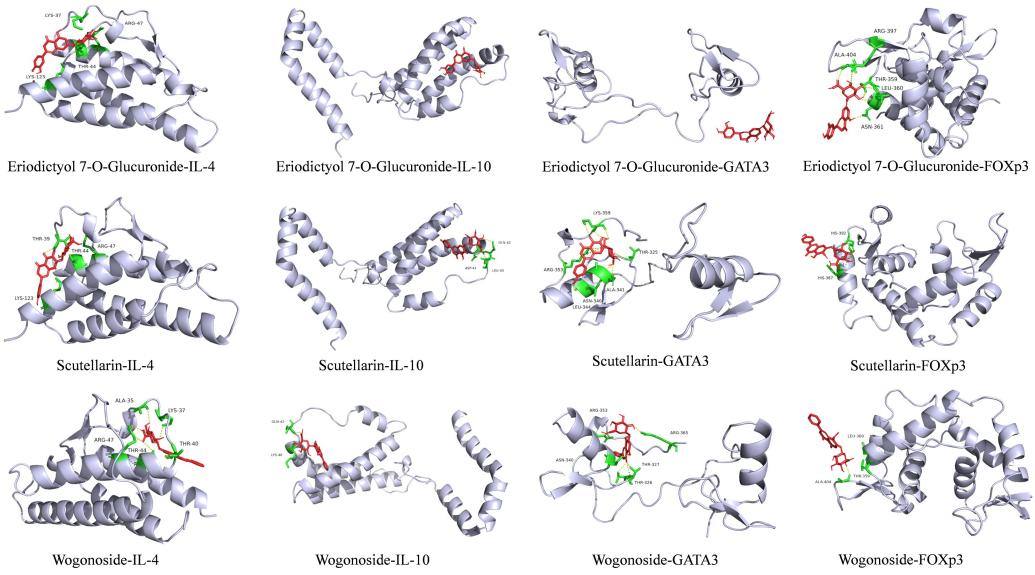

Figure 8 Molecular docking model of core compounds and targets

Network pharmacology is an emerging approach in biological research and drug discovery and research rooted in modeling and simulation and large-scale data collection and analysis, which can facilitate drug discovery, predict targets, and predict the mechanism of action of drugs in preclinic [34–36]. Network pharmacology was employed to investigate the active compounds, targets, and pathways of drugs or prescriptions acting on diseases at the molecular level to promote the development of drug research and development. In this study, we identified the major targets of WQY for AD treatment and investigated its potential structural, molecular, and cellular functional panels and associated pathways, and constructed the WQY-compounds-targets-disease network to elucidate the network regulatory mechanism of WQY in AD therapy. The study demonstrated that WQY possesses the potential to treat AD by modulating Toll-like receptor and T-cell receptor signaling pathways, as well as influencing the differentiation pathways of Th1 and Th2 cells.

Extensive research has demonstrated that the development of AD is closely associated with T cells, and during the pathogenesis period, significant fluctuations in the levels of Th1 (IFN-γ), Th2 (IL-4, IL-13), Th17 (IL-17), and Treg (IL-10) cytokines had been observed [37–39]. At the outset of AD, therapeutic objectives can be met by reducing the levels of cytokines such as IL-4, IL-13, and IL-10 [40]. It was found that WQY significantly decreased the expression of IL-4, IL-10, GATA3 and FOXP3 in AD mice, and negligible changes were observed in the mRNA levels of IFN-γ, IL-17, T-bet and RORγ. Previous studies have shown that both the acute and chronic stages of Alzheimer's disease are marked by elevated levels of Th2 cytokines, such as IL-4, which either impede filaggrin expression or inhibit mast cell degranulation [41]. The role of Treg in the pathogenesis of AD, particularly in chronic AD, is significant as Treg cells dominate and exert immunosuppressive effects through cytokine production [42]. Inhibition of mast cell infiltration, IgE and proinflammatory factors by Treg cells immune response can improve the sensitization and induction of AD pathogenesis [43]. In addition, Treg cells can promote Th2 immune responses, and the pathway is bidirectional [44]. Thus, the mechanism of WQY in treating AD may involve suppressing Th2 and Treg cells immune response.

To further explore the potential functional components of WQY, molecular docking experiments were performed. The study results indicated that eriodictyol 7-O-glucuronide, scutellarin, wogonoside, and rhaponticin were potential functional components. Scutellarin possesses antioxidant and anti-inflammatory properties, and it effectively reduces the number of Treg cells while inhibiting their activity, ultimately enhancing immune function [45, 46]. Wogonoside was found to reduce the expression of IL-13, an inflammatory factor secreted by Th2 cells in mice with colitis, to maintain the immune homeostasis of the intestine [47]. To investigate the anti-inflammatory properties of rhapontin, an inflammation model was established in mice, and the results revealed that rhapontin markedly attenuated the levels of inflammatory factors [48]. Additionally, rhapontin decreased TGF-β1 expression by inhibiting the TGF-β/Smad pathway [49]. The above ingredients screened through network pharmacology and molecular docking analysis are likely to be the effective ingredients of WQY in regulating Th2 and Treg cells immune response to treat AD, which are worthy of further exploration in future studies.

Conclusion

In this study, we examined the effects and underlying mechanisms of WQY on AD with a DNFB-induced mouse model. The results demonstrated that WQY effectively mitigated tissue damage, reduced inflammatory factors levels, and regulated the balance of $CD4^+$ and $CD8^+$ cells in AD mice. By employing UPLC-Orbitrap-MS/MS technique and constructing a drug target network, potential active ingredients such as coumestrol, muricarpone B, luteolin, wogonin, glaucine were identified. Furthermore, network pharmacology and qRT-PCR analysis, in conjunction with molecular docking, have confirmed that the mechanism by which WQY exerts its therapeutic effects on AD may be associated with the inhibition of Th2 and Treg cell immune responses. Additionally, compounds such as eriodictyol 7-O-glucuronide, scutellarin, wogonoside, among others, may serve as potential active components within WQY.

References

1. Yao TC, Wang IJ, Sun HL, et al. Taiwan guidelines for the diagnosis and management of pediatric atopic dermatitis: Consensus statement of the Taiwan Academy of Pediatric Allergy, Asthma and Immunology. *J Microbiol Immunol Infect*. 2022;55(4):561–572. Available at: http://doi.org/10.1016/j.jmii.2022.03.004
2. Bieber T. Atopic dermatitis. *N Engl J Med*. 2008;358(14):1483–1494. Available at: http://doi.org/10.1056/NEJMra074081
3. Darbà J, Marsà A. Atopic dermatitis in specialized centers in Spain: a retrospective analysis of incidence and costs (2000–2017). *Expert Rev Pharmacoecon Outcomes Res*. 2021;21(4):737–742. Available at: http://doi.org/10.1080/14737167.2021.1823222
4. Chan LN, Magyari A, Ye M, et al. The epidemiology of atopic dermatitis in older adults: A population-based study in the United Kingdom. *PLoS One*. 2021;16(10):e0258219. Available at: http://doi.org/10.1371/journal.pone.0258219
5. Bélanger É, Madore AM, Boucher-Lafleur AM, et al. Eosinophil microRNAs Play a Regulatory Role in Allergic Diseases Included in the Atopic March. *Int J Mol Sci*. 2020;21(23):9011. Available at: http://doi.org/10.3390/ijms21239011
6. Chong M, Fonacier L. Treatment of Eczema: Corticosteroids and Beyond. *Clin Rev Allergy Immunol*. 2016;51(3):249–262. Available at: https://pubmed.ncbi.nlm.nih.gov/25869743/
7. Yuan HM, Tang Y, Zhang SJ, et al. NLRP3 neuroinflammatory intervention of Mahuang-Lianqiao-Chixiaodou decoction for mental disorders in atopic dermatitis mice. *J Ethnopharmacol*. 2024;319(Pt 2):117263. Available at: http://doi.org/10.1016/j.jep.2023.117263
8. Xie LP, Zhou CY, Wu YT, et al. Wenqingyin suppresses ferroptosis in the pathogenesis of sepsis-induced liver injury by activating the Nrf2-mediated signaling pathway. *Phytomedicine*. 2023;114:154748. Available at: http://doi.org/10.1016/j.phymed.2023.154748
9. Qing CZ, Shi JS. Clinical study of Wenqingyin in the treatment of atopic dermatitis. *China Foreign Med Treat*. 2008;12:55–56. (Chinese).
10. Yin ZJ, Su Q. Wenqingyin Treats Various Skin Diseases. *Inner Mong J Tradit Chin Med*. 1997;1:16. (Chinese) Available at: http://doi.org/10.16040/j.cnki.cn15-1101.1997.01.012
11. Cai QF. Preparation and clinical application of Kampo preparation Wenqingyin ointment. *Chin Tradit Patent Med*. 1996;2:49. (Chinese).
12. Che W. Clinical retrospective summary of Wenqingyin in the treatment of atopic dermatitis. Beijing University of Chinese Medicine. 2005. (Chinese).
13. Kim S, Chen J, Cheng TJ, et al. PubChem in 2021: new data content and improved web interfaces. *Nucleic Acids Res*. 2021;49(D1):D1388–D1395. Available at: http://doi.org/10.1093/nar/gkaa971
14. Daina A, Michielin O, Zoete V. Swiss Target Prediction: updated data and new features for efficient prediction of protein targets of small molecules. *Nucleic Acids Res*. 2019;47(W1):W357–W364. Available at: http://doi.org/10.1093/nar/gkz382
15. Wishart DS, Feunang YD, Guo AC, et al. DrugBank 5.0: a major update to the DrugBank database for 2018. *Nucleic Acids Res*. 2018;46(D1):D1074–D1082. Available at:

http://doi.org/10.1093/nar/gkx1037
16. Fishilevich S, Nudel R, Rappaport N, et al. GeneHancer: genome-wide integration of enhancers and target genes in GeneCards. *Database (Oxford)*. 2017;2017:bax028. Available at: http://doi.org/10.1093/database/bax028
17. Amberger JS, Bocchini CA, Scott AF, et al. OMIM.org: leveraging knowledge across phenotype-gene relationships. *Nucleic Acids Res*. 2019;47(D1):D1038–D1043. Available at: http://doi.org/10.1093/nar/gky1151
18. UniProt Consortium. UniProt: the universal protein knowledgebase in 2021. *Nucleic Acids Res*. 2021;49(D1):D480–D489. Available at: http://doi.org/10.1093/nar/gkaa1100
19. Oliveros JC. Venny. An interactive tool for comparing lists with Venn Diagrams. 2007. Available at: https://bioinfogp.cnb.csic.es/tools/venny/index.html
20. Szklarczyk D, Kirsch R, Koutrouli M, et al. The STRING database in 2023: protein-protein association networks and functional enrichment analyses for any sequenced genome of interest. *Nucleic Acids Res*. 2023;51(D1):D638–D646. Available at: http://doi.org/10.1093/nar/gkac1000
21. Che YH, Xu ZR, Ni LL, et al. Isolation and identification of the components in Cybister chinensis Motschulsky against inflammation and their mechanisms of action based on network pharmacology and molecular docking. *J Ethnopharmacol*. 2022;285:114851. Available at: http://doi.org/10.1016/j.jep.2021.114851
22. Zhou Y, Zhou B, Pache L, et al. Metascape provides a biologist-oriented resource for the analysis of systems-level datasets. *Nat Commun*. 2019;10(1):1523. Available at: http://doi.org/10.1038/s41467-019-09234-6
23. Li XJ, Xiao Z, Pu WY, et al. Network pharmacology, molecular docking, and experimental validation to explore the potential mechanism of Long Mu Qing Xin mixture for the treatment of attention deficit hyperactivity disorder. *Front Pharmacol*. 2023;14:1144907. Available at: http://doi.org/10.3389/fphar.2023.1144907
24. O'Boyle NM, Banck M, James CA, et al. Open Babel: An open chemical toolbox. *J Cheminform*. 2011;3:33. Available at: http://doi.org/10.1186/1758-2946-3-33
25. Berman HM, Westbrook J, Feng Z, et al. The Protein Data Bank. *Nucleic Acids Res*. 2000;28(1):235–242. Available at: http://doi.org/10.1093/nar/28.1.235
26. Trott O, Olson AJ. AutoDock Vina: improving the speed and accuracy of docking with a new scoring function, efficient optimization, and multithreading. *J Comput Chem*. 2010;31(2):455–461. Available at: http://doi.org/10.1002/jcc.21334
27. Wang SJ, Liu QQ, Jiang HJ, et al. Active components and mechanism of Taohong Siwu Decoction in treatment of primary dysmenorrhea based on network pharmacology and molecular docking technology. *Chin J Chin Mater Med*. 2020;45(22):5373–5382. (Chinese) Available at: http://doi.org/10.19540/j.cnki.cjcmm.20200723.401
28. Gao FY, Liu T, Zhang ZH, et al. Research progress on the pathogenesis of ulcerative colitis and the intervention of Traditional Chinese medicine based on NF-κB pathway. *Chin Arch Tradit Chin Med*. 2023;41(6):123–127. (Chinese) Available at: http://doi.org/10.13193/j.issn.1673-7717.2023.06.026
29. Choi YA, Yu JH, Jung HD, et al. Inhibitory effect of ethanol extract of Ampelopsis brevipedunculata rhizomes on atopic dermatitis-like skin inflammation. *J Ethnopharmacol*. 2019;238:111850. Available at: http://doi.org/10.1016/j.jep.2019.111850
30. Song JY, Kang HJ, Ju HM, et al. Umbilical cord-derived mesenchymal stem cell extracts ameliorate atopic dermatitis in mice by reducing the T cell responses. *Sci Rep*. 2019;9(1):6623. Available at: http://doi.org/10.1038/s41598-019-42964-7
31. Verde MT, Villanueva-Saz S, Loste A, et al. Comparison of circulating $CD4^+$, $CD8^+$ lymphocytes and cytokine profiles between dogs with atopic dermatitis and healthy dogs. *Res Vet Sci*. 2022;145:13–20. Available at: http://doi.org/10.1016/j.rvsc.2022.01.018
32. Fan P, Xie S, Zhang Z, et al. Polygonum perfoliatum L. ethanol extract ameliorates 2,4-dinitrochlorobenzene-induced atopic dermatitis-like skin inflammation. *J Ethnopharmacol*. 2024;319(Pt 2):117288. Available at: https://pubmed.ncbi.nlm.nih.gov/37827300/
33. Leung KS, Fong BM. LC-MS/MS in the routine clinical laboratory: has its time come? *Anal Bioanal Chem*. 2014;406(9–10):2289–2301. Available at: http://doi.org/10.1007/s00216-013-7542-5
34. Vicini P, van der Graaf PH. Systems pharmacology for drug discovery and development: paradigm shift or flash in the pan? *Clin Pharmacol Ther*. 2013;93(5):379–381. Available at: http://doi.org/10.1038/clpt.2013.40
35. Zhou W, Wang YH, Lu AP, et al. Systems Pharmacology in Small Molecular Drug Discovery. *Int J Mol Sci*. 2016;17(2):246. Available at: http://doi.org/10.3390/ijms17020246
36. Pérez-Nueno VI. Using quantitative systems pharmacology for novel drug discovery. *Expert Opin Drug Discov*. 2015;10(12):1315–1331. Available at: http://doi.org/10.1517/17460441.2015.1082543
37. Tsiogka A, Kyriazopoulou M, Kontochristopoulos G, et al. The JAK/STAT Pathway and Its Selective Inhibition in the Treatment of Atopic Dermatitis: A Systematic Review. *J Clin Med*. 2022;11:4431. Available at: http://doi.org/10.3390/jcm11154431
38. Hou T, Sun X, Zhu J, et al. IL-37 Ameliorating Allergic Inflammation in Atopic Dermatitis Through Regulating Microbiota and AMPK-mTOR Signaling Pathway-Modulated Autophagy Mechanism. *Front Immunol*. 2020;11:752. Available at: http://doi.org/10.3389/fimmu.2020.00752
39. Bieber T. Interleukin-13: Targeting an underestimated cytokine in atopic dermatitis. *Allergy*. 2020;75(1):54–62. Available at: http://doi.org/10.1111/all.13954
40. Lee Y, Choi HK, N'deh KPU, et al. Inhibitory Effect of Centella asiatica Extract on DNCB-Induced Atopic Dermatitis in HaCaT Cells and BALB/c Mice. *Nutrients*. 2020;12(2):411. Available at: http://doi.org/10.3390/nu12020411
41. Hou DD, Gu YJ, Wang DC, et al. Therapeutic effects of myricetin on atopic dermatitis in vivo and in vitro. *Phytomedicine*. 2022;102:154200. Available at: http://doi.org/10.1016/j.phymed.2022.154200
42. Jia JJ, Mo XM, Yan FG, et al. Role of YAP-related T cell imbalance and epidermal keratinocyte dysfunction in the pathogenesis of atopic dermatitis. *J Dermatol Sci*. 2021;101(3):164–173. Available at: http://doi.org/10.1016/j.jdermsci.2020.12.004
43. Kang LJ, Oh E, Cho C, et al. 3'-Sialyllactose prebiotics prevents skin inflammation via regulatory T cell differentiation in atopic dermatitis mouse models. *Sci Rep*. 2020;10(1):5603. Available at: http://doi.org/10.1038/s41598-020-62527-5
44. Nedoszytko B, Lange M, Sokołowska-Wojdyło M, et al. The role of regulatory T cells and genes involved in their differentiation in pathogenesis of selected inflammatory and neoplastic skin diseases. Part II: The Treg role in skin diseases pathogenesis. *Postepy Dermatol Alergol*. 2017;34(5):405–417. Available at: http://doi.org/10.5114/ada.2017.71105
45. Zhang X, Dong ZC, Fan H, et al. Scutellarin prevents acute alcohol-induced liver injury via inhibiting oxidative stress by regulating the Nrf2/HO-1 pathway and inhibiting inflammation by regulating the AKT, p38 MAPK/NF-κB pathways. *J Zhejiang*

Univ Sci B. 2023;24(7):617–631. Available at: http://doi.org/10.1631/jzus.B2200612

46. Chen S, Li R, Chen Y, et al. Scutellarin enhances anti-tumor immune responses by reducing TNFR2-expressing $CD4^+FOXP3^+$ regulatory T cells. *Biomed Pharmacother*. 2022;151:113187. Available at: http://doi.org/10.1016/j.biopha.2022.113187
47. Huang SW, Fu YJ, Xu B, et al. Wogonoside alleviates colitis by improving intestinal epithelial barrier function via the MLCK/pMLC2 pathway. *Phytomedicine*. 2020;68:153179. Available at: http://doi.org/10.1016/j.phymed.2020.153179
48. Eräsalo H, Hämäläinen M, Leppänen T, et al. Natural Stilbenoids Have Anti-Inflammatory Properties in Vivo and Down-Regulate the Production of Inflammatory Mediators NO, IL6, and MCP1 Possibly in a PI3K/Akt-Dependent Manner. *J Nat Prod*. 2018;81(5):1131–1142. Available at: http://doi.org/10.1021/acs.jnatprod.7b00384
49. Tao LJ, Cao J, Wei WC, et al. Protective role of rhapontin in experimental pulmonary fibrosis in vitro and in vivo. *Int Immunopharmacol*. 2017;47:38–46. Available at: http://doi.org/10.1016/j.intimp.2017.03.020